354 *Macromolecules* **2010**, *43*, 354–361
DOI: 10.1021/ma9020856

Macromolecules
ARTICLE

In Situ Follow-Up of the Intercalation Process in a Clay/Polymer Nanocomposite Model System by Rheo-XRD Analyses

A. Reyna-Valencia,[†] Y. Deyrail,[†] and M. Bousmina*[,†,‡,§]

[†]*Department of Chemical Engineering, Laval University, Quebec, Canada G1K 7P4, Canada Research Chair on Polymer Physics and Nanomaterials,* [‡]*INANOTECH (Institute of Nanomaterials and Nanotechnology), Rabat, Morocco, and* [§]*Hassan II Academy of Science and Technology, Rabat, Morocco*

Received September 22, 2009; Revised Manuscript Received November 21, 2009

ABSTRACT: This work deals with the follow-up of structure evolution in clay−polymer nanocomposites during the intercalation process through *in situ* analyses combining X-ray diffraction and rheology using a home-modified X-ray diffraction setup coupled with a rheometer with a special shearing cell developed for this work. To avoid any interference of medium elasticity, the selected matrix was a bisphenol A-based epoxy resin DGEBA with a Newtonian behavior under the examined experimental conditions. The selected clay was an organophilic montmorillonite (Cloisite 30B). The evolution of clay stacks in the clay−polymer nanocomposites was assessed under quiescent conditions by simultaneous time-resolved X-ray diffraction (XRD) and rheometry. The main results showed a very slow polymer diffusion process that increases the concentration of the intercalated stacks, narrows their distribution, and decreases the number of lamellae per stack.

1. Introduction

The use of nanoscopic clay particles as additives in a polymer matrix has been found to enhance various performances and to provide advantageous properties to the neat resin including reduced permeability and flammability, enhanced thermal stability and colorability, and to some extent enhanced mechanical properties, without changing much the density and the optical transparency of the hosting polymer matrix. These effects are obtained through dispersion/distribution and full or partial exfoliation of the clay lamellae within the polymer matrix. From industrial perspectives, the preferred route for preparing polymer nanocomposites (PNCs) with thermoplastic matrixes is the melt-mixing of the polymer with surfactant-intercalated clay particles using classical processing tools such as extrusion and batch mixing. Dispersion, delamination, and distribution of the clay lamellae are promoted by the combined effect of diffusion and mechanical deformation through shear or extensional flow,[1] provided that the organic clay intercalant is thermally stable and presents peculiar specific interactions with the polymer matrix.

The optimum melt-mixing conditions for controlling the evolution of the structure in PNCs and obtaining a high degree of dispersion, exfoliation, and homogeneous distribution are still a matter of debate. Considerable experimental research has been devoted to investigate the influence of melt compounding variables on the final structure of commonly studied systems based on polyamide-6 or polypropylene[2−10] and other polyolefin-based matrices.[11] The exfoliation degree has been related to the shearing conditions such as the stress level—related to the applied shear rate and to the matrix viscosity (molecular weight)—and the total strain or deformation—dependent on the mixing time. Bousmina[11] carried out an analysis of the fundamental physics involved in mechanical exfoliation supported by experimental data and concluded that the highest exfoliation level and the best associated mechanical properties result from the balance between the polymer chain diffusion within the clay galleries and mechanical stresses. While the former is favored by low matrix viscosity, the latter requires highly viscous matrices. In any case, high level of exfoliation is obtained only if the first step of diffusion is allowed to take place. That is, medium matrix viscosity and mild shearing conditions to facilitate diffusion followed by higher applied shear for increasing delamination are required. One of the main conclusions of the above study is that full exfoliation is not always needed to enhance the mechanical properties of the hosting matrix, and the required level of exfoliation depends on the flexibility−rigidity and thermal behavior (thermoplastics versus thermosets) of the used polymer matrix.

The structural properties developed in either the extruder or the batch mixer have been typically characterized via postmortem tests, i.e., separated rheological and X-ray diffraction measurements along with afterward transmission electron microscopy (TEM) analyses. This means that the morphology assessed by X-ray and TEM analyses is assumed to be the same as that revealed by indirect rheological measurements. Such assumption might be in some cases not adequate due to time evolution of the structure that generates different clay dispersion−distribution in the samples used in the various analyses.

This work is aimed at studying *in situ* the intercalation process and the structure development in a polymer matrix mixed with clay nanoparticles using a home-developed X-ray diffraction setup coupled with a rheometer. Such a setup allows direct and *in situ* analyses of the clay structure during shearing. The aim here is to study how the structure evolves over time under quiescent conditions during the intercalation process. The experimental methodology consists in tracking structural development *in situ* by simultaneous time-resolved X-ray diffraction (XRD) and small-amplitude oscillatory shear flow.

On one hand, rheometry is a useful quantitative technique for sensing the evolution of the structure from the macro- to the meso- and nanoscales, and on the other hand, the X-ray scattering technique is able to assess the ordering and the evolution of

*Corresponding author: E-mail: m.bousmina@inanotech.ma.

 Published on Web 12/07/2009

the interlayer distance in clay stacks. By coupling rheological tests and online XRD measurements, a portrait of morphology development can be obtained by relating the changes in rheological material functions to the changes in clay stacks caused by clay dispersion/distribution. In this way, experimental variables such as time, applied deformation, or shear stress values (depending on shearing conditions and on the matrix properties) can be associated with different states of structural development.

To the best of our knowledge, hitherto only an extremely limited number of papers have been published using coupled rheometry with online XRD setup to obtain complete structural information on nanoclay-filled polymers.[11−13] In particular, Homminga et al.[13] observed that shear forces cause the initial breakup of clay agglomerates, but their role in further exfoliation is limited. Bousmina[11] found that the state of clay dispersion−delamination and distribution may evolve over time depending on the matrix viscosity and on the matrix−clay interfacial interactions; moreover, such time-dependent evolution is a function of shear history. The above-mentioned studies highlight the importance of clarifying the fundamental aspects of structural development, which is the aim of the present research.

In summary, this paper reports on the *in situ* characterization of structure development during the intercalation process in PNCs using rheometry coupled with XRD. Structural evolution has been studied under quiescent conditions using a model polymer with no elastic stresses (Newtonian matrix) that may contribute to the overall stress in the system. The Experimental Section provides details on the homemade shearing system developed for this work. The Results and Discussion section presents a summary on the collected XRD and rheology data and integrates the information obtained from both sources to discuss the mechanism of intercalation and to yield a portrait of structure development.

2. Experimental Section

2.1. Materials and Sample Preparation. The polymer model used in this work is an epoxy resin diglycidyl ether of bisphenol A (DGEBA), commercially available as Epon 828 from Shell Chemical. It is characterized by a number-average molecular weight (M_n) of 411 g/mol, and a viscosity of 7 Pa·s at room temperature (28 °C), and a glass transition temperature of −14 °C. At room temperature, DGEBA is liquid, does not absorb significantly the X-rays, and has no elasticity (Newtonian matrix) that may interfere with data interpretation. The employed layered silicate employed is the organically modified montmorillonite clay (Cloisite 30B) from Southern Clay Products, with methyl tallow bis(2-hydroxyethyl) quaternary ammonium as surfactant in a concentration of 90 mequiv/100 g. Figure 1 shows the chemical structures of DGEBA and the clay surfactant used to modify the virgin montmorillonite; this compound has a hydroxyl group that interacts with the epoxy group of the matrix.

Samples containing 1.5−10 wt % of nanoclay were prepared by manually dispersing manually the particles in the molten polymer at room temperature. The PNCs were loaded immediately in the measuring cell of the rheometer and tested within 5 min after initial contact between the components after a preshear of 30 s at 10 s^{-1}. Such preshear conditions were found to induce reproducible initial morphological characteristics.

2.2. Techniques. X-ray diffraction is the most popular technique to study intercalation/exfoliation of clay lamellae in polymeric matrices by measuring the interlamellar distance of the clay ordered structure. When X-rays (typical wavelength of about 0.1 nm) strikes an ordered structure with regularly spaced arrays of atoms, the waves are scattered in different directions (different angles) with respect to the incident beam. The time-averaged scattered intensity is measured as a function of the scattering angle. The analysis of the position and intensity of diffraction peaks provides information about the *d*-spacing and

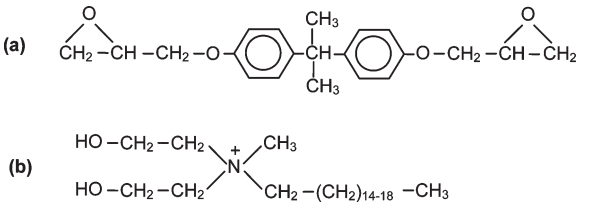

Figure 1. Chemical structures of (a) DGEBA and (b) clay surfactant methyl tallow bis(2-hydroxyethyl)ammonium.

on the spatial arrangement of the clay lamellae within the polymer matrix. The intensity of diffraction maxima depends on the periodicity and the concentration of the scattering units, i.e., the number and regularity of repeating individual elements that scatter waves coherently.

For clay stacks, the spacing between lamellae is calculated from the angles at which diffraction maxima occur according to Bragg's law: $d = \lambda/2 \sin \theta$, where d is the interplanar distance, λ is the wavelength of radiation (Cu Kα radiation of 1.542 Å), and θ is the diffraction angle. Pure montmorillonite clay with Na^+ cations in the interlayer space diffracts X-rays at an angle of about $2\theta = 9°-11°$, corresponding to a gallery height of about 1 nm. In polymer/clay nanocomposites, the shift in the diffraction peak to lower angles is associated with the expansion of the interlamellar spacing (intercalation). A fully exfoliated structure is usually indicated by the absence of the diffraction peak in the angular region $1° \leq 2\theta \leq 10°$. When the interlayer distance becomes larger than the characteristic length of the polymer chains (gyration radius or end-to-end distance), the diffusion process is likely to take place, helping the polymeric chains to penetrate into the clay galleries and push them apart by a thermally favored randomization mechanism.[11] The peak intensity and its location may be affected by local concentration in the sample, and thus one should be aware of partial exfoliation and inhomogeneous distribution. The technique is not infallible, and its drawbacks must be taken into account for rigorous interpretation of the results.

The rheometer serves two purposes in this work: as a device to generate controlled flow conditions and as a characterization tool to assess the structure evolution under quiescent conditions due to either structure build-up or loss of structure by thermally driven Brownian motion. The main analysis is based on examining simultaneously the time evolution of the peak location and its intensity along with the evolution of the rheological material functions that reveal the molecular mobility and the short- or long-range structure build-up. Clay dispersion, intercalation−exfoliation, and distribution affect molecular motion due to the increase in the interface between the matrix and the clay particles, thus modifying the molecular relaxation of the polymer matrix. Such effect is enhanced by polymer−lamellae interactions, by colloidal interactions occurring between the clay stacks, and by the increased surface area of clay.

Therefore, different rheological signatures are obtained for intercalated, partially or fully exfoliated lamellae, and homogeneous versus inhomogeneous dispersion. The scope of this work is restricted to the intercalation process under quiescent conditions, and therefore the response obtained for small-amplitude oscillatory shear flow is examined only at medium frequency is examined.

2.3. Experimental Setup. The setup for studying *in situ* structure evolution in polymer nanocomposites by simultaneous XRD and rheometry was described elsewhere.[11] In short, it consists of a Bruker D8 AXS X-ray diffractometer coupled with an Anton Paar MCR501 rheometer and a transparent Couette cell as shown in Figure 2. A special homemade shearing cell was developed for the present study and consists of two coaxial cylinders (a driven bob and a stationary cup) made of poly(methyl methacrylate) with a stainless steel shaft (Figure 3). The design of this cell took into account several criteria. The

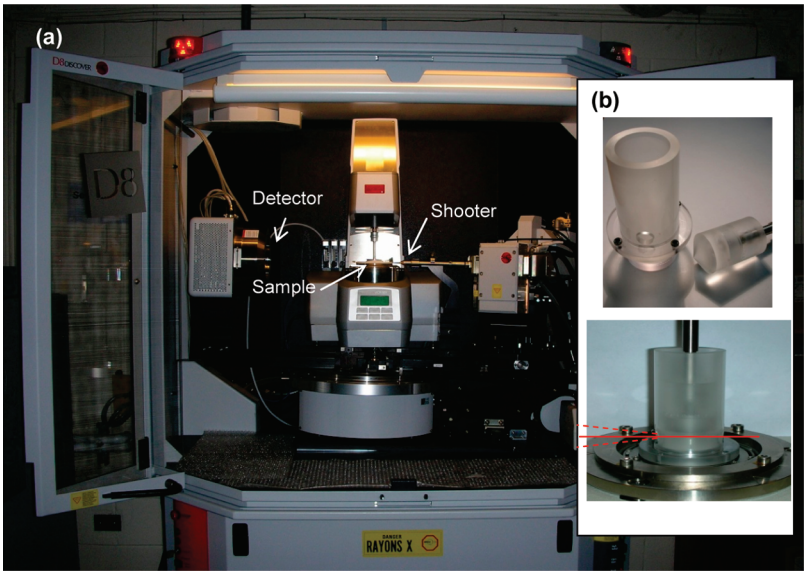

Figure 2. (a) Rheo-XRD experimental setup: Anton Paar's Physica MCR rheometer + Bruker's D8 XRD system. (b) Homemade coaxial cylinders measuring device.

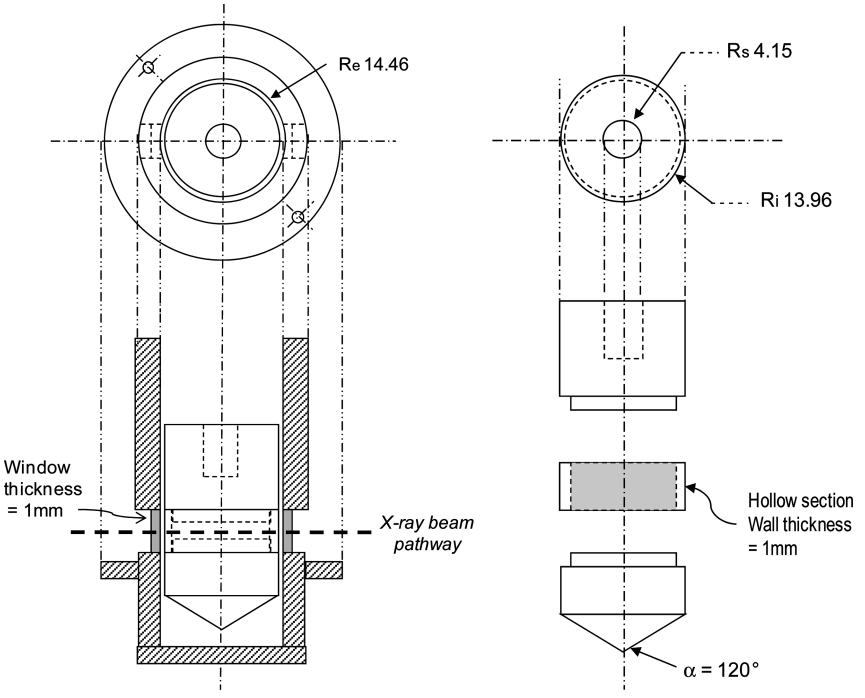

Figure 3. Coaxial cylinder measuring system: (a) external cylinder (cup), (b) internal cyclinder (bob). Radii in mm. Design and drawings by A. Reyna-Valencia.

construction material had to be transparent to X-rays and easy to machine. To reduce the absorption of radiation, the bob was assembled in several parts and included a hollow section aligned with the beam direction. Correspondingly, the cup had two windows of reduced thickness. Absorption tests provided the tolerated thicknesses of both the cell walls and the sample to reduce parasite absorption and obtain clear diffraction patterns with an ordinary beam at the shortest acquisition time. The system dimensions were then adjusted to rheological specifications (ASTM norms), and correction of inertia was done accordingly. The resulting system allows the rheometer to be fully functional, while working in the configuration radiation source−rheometer−detector. Other online rheo-XRD setups reported in the literature involve more complex shearing devices and were developed for use in synchrotron lines.[13−15] In contrast, the setup described here has been engineered in a more simple way and was developed for the classical XRD facilities available in university laboratories.

2.4. Methodology. In a typical test sequence, a preshear of 30 s at 10 s^{-1} was applied at the start of the experimental protocol to erase previous shear history and to ensure reproducible initial conditions.[16−18] Afterward, XRD and rheological data were collected simultaneously. Time sweep experiments were carried out to follow the structure build-up at rest. In this kind of SAOS tests, both the amplitude and the frequency of deformation were held constant, and the time evolution of the dynamic moduli was measured. The amplitude of deformation was low enough so as the structure of the sample was unaffected by the test conditions (preliminary strain sweep experiments provided the acceptable range of amplitudes of deformation). At the end of the

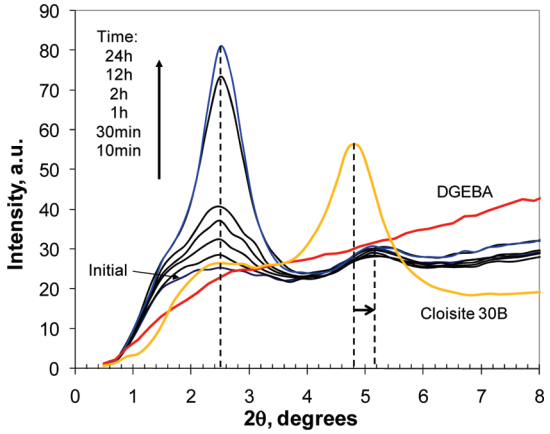

Figure 4. Time-resolved evolution of diffracted intensity for a Cloisite 30B/DGEBA PNC containing a clay fraction of 5 wt %. Data obtained at room temperature.

experiment of an average duration of 12 h, the rheological signature of the structure developed by each PNC was obtained through a frequency sweep test. The SAOS test probes the PNC structure in the linear viscoelastic range: at high frequencies the behavior is governed by the molten polymer, while at low frequencies the response is sensitive to the state of dispersion−delamination and distribution of the solid phase within the polymer matrix. The medium frequency range is suitable for studying the polymer chain dynamics in the presence of organoclay and therefore the intercalation process, which is the aim of the present work. The rheo-XRD data were then integrated to propose a portrait of structure development in organoclay/DGEBA systems.

The XRD measurements were performed in a 2θ range between 0.5° and 10° with an acquisition time of 90 s with radiation generated at 45 kV and 100 mA.

3. Results and Discussion

3.1. XRD Data. Figure 4 shows the time-resolved XRD data obtained for pure Cloisite 30B and for a PNC with 5 wt % of Cloisite 30B. The results reveal several peculiar features. First, the pure Cloisite 30B displays a major sharp peak at about $2\theta = 4.9°$, corresponding to a gallery height of 1.8 nm, as well as an ill-defined broad peak of low intensity at $2\theta = 2.5°$, corresponding to an average equivalent *d*-spacing of about 3.5 nm. The first peak corresponds to a *d*-spacing that is in agreement with the data provided by the supplier ($d_{001} = 1.85$ nm) and the data published in the literature. However, the second broad peak is unusual and may suggest that the particular batch of Cloisite 30B used in this work consisted of montmorillonite clay modified with a nonhomogeneous surfactant. In general, the surfactant used to modify the pure montmorillonite for producing commercial Cloisite 30B consists of MT2EtOH: methyl, tallow, bis(2-hydroxyethyl) quaternary ammonium, where the tallow T is a mixture of aliphatic chains having the following proportion: ~65% C18; ~30% C16; ~5% C14. The results obtained in this work suggest that the particular batch used for sample preparation involves other eventual mixtures of T with a higher number of carbons, giving rise to the small portion of organoclay with a larger *d*-spacing ($d = 3.5$ nm).

Second, upon incorporation of Cloisite 30B to the polymeric matrix, the large sharp peak of the pure organoclay at $2\theta = 4.9°$ disappears and is replaced by a much smaller peak at 5.1°, which is only slightly more intense than the peak at 2.5° discussed above for the neat Cloisite 30B. Over time, this peak remains more or less unchanged, while the peak of the PNC at 2.5° becomes more intense, sharper, and better resolved.

In previous studies about PNCs, the secondary peak at high angles is usually not mentioned in the discussion, though it is visible in the graphs. Some authors attributed it to a "second reflection" of the primary peak[4] or considered it as an "interference" peak.[19] A secondary peak was also observed by Kong and Park[20] for octadecylamine-treated clay in DGEBA and attributed it to nonintercalated stacks.

Two possible mechanisms may be evoked to explain the observed peak at higher 2θ values in PNCs. The first one is that the peak at 5.1° might correspond to a small fraction of the organoclay that has not been uniformly modified by the surfactant and is therefore not amenable to intercalation by the polymeric chains. The second possibility can be attributed to the existence of a more favorable *d*-spacing at $2\theta = 2.5°$, which offers more open clay galleries to the diffusing polymer chains. Therefore, the polymer chains tend to intercalate the galleries diffracting at $2\theta = 2.5°$ rather than the ones at $2\theta = 4.9°$ because diffusion inside the open galleries requires a lower energy cost (higher entropy) than diffusion in smaller channels corresponding to $2\theta = 4.9°$ that has been shifted to 5.1°. The result is a growth in the peak intensity at 2.5°, which translates into an increase in the intercalated organoclay stacks corresponding to $2\theta = 2.5°$, and a shift of the Cloisite 30B sharp peak at $2\theta = 2.49°$ to $2\theta = 2.51°$, implying a shrink of the structure and a decrease in the interlamellar spacing. Such a decrease in *d*-spacing in the presence of the polymer may be related to the increase in the concentration of the intercalated stacks that push away the matrix polymeric chains that are not involved in the intercalation process, which in turn squeeze the polymer-free organoclay stacks. The surfactant within such squeezed stacks changes orientation and becomes more oriented parallel to the clay surface.

Kádár et al.[19] evaluated the gap occupied by two surfactant molecules that lay parallel inside the gallery and found that it corresponds to a height ranging from 1.7 to 2 nm ($2\theta = 4.9°-5.2°$), approximately. Consequently, that would be the maximum interlayer spacing allowed for organically modified clay stacks immersed in a polymer medium. Our results show a secondary peak that seems to remain unchanged over time. In contrast, Kong and Park[20] reported that the initial XRD frame displays one single peak corresponding to nonintercalated clay; 6 min later the primary peak started to develop and during the test the primary peak grew, while the second peak decreased. Our first frame was obtained after 6 min of PNC preparation, and at this time, the second peak had already reached its final intensity even if the primary peak was just starting to develop. Probably our system is characterized by better specific interactions between the hydroxyl groups of the surfactant molecules and the expoxy group of the matrix, which would explain the changes observed at room temperature, whereas Kong and Park had to work at 50 °C and did not see any change at room temperature.

Another feature of the PNC diffraction pattern is the appearance of a shoulder on the main peak at 2.5°. This might be attributed to a distribution of the gallery spacing that appear at multiple diffraction angles. With time, such distribution narrows down to an apparent equilibrium value as evidenced by the peak that becomes sharper and more resolved. In fact, the width at midheight is related to the number of lamellae within the stacks, and the intensity height and the surface under the peak are related to stack intensity. The obtained data mean that the number of stacks increases, while the number of lamellae per stack is decreasing.

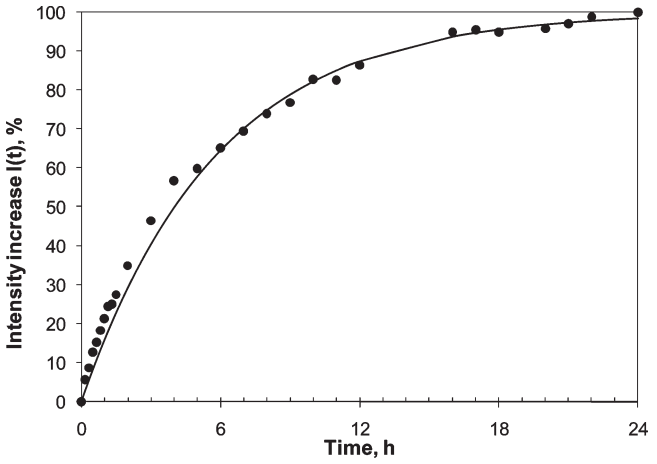

Figure 5. Growth of the diffracted-intensity peak located at $2\theta = 2.5°$ over time for the 5 wt % clay PNC (data from Figure 4 transformed according to eq 1). Full symbols indicate the experimental points, and the solid line is the curve fitting obtained through eq 2.

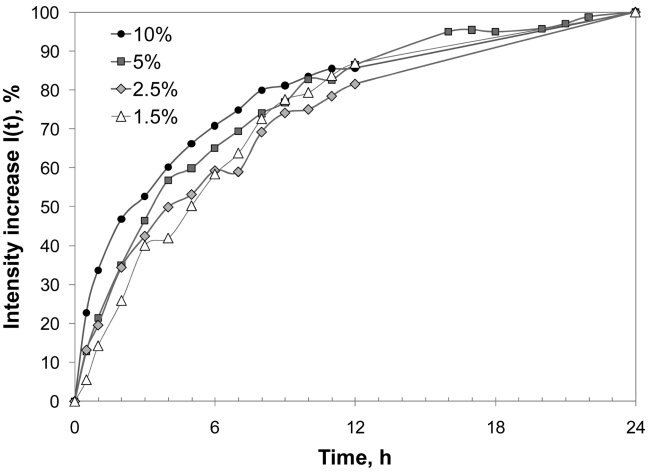

Figure 6. Evolution of the intensity peak at $2\theta = 2.5°$ over time for samples with different clay concentrations (in wt %). The lines are for guiding the eye.

The analysis of the intensity of the primary peak requires data normalization to allow comparison between samples; for this purpose, only the value of the highest point of the curve is taken into account. The width at half height was not considered in our analysis because peak profiles were ill-defined during a significant part of the process (< 6 h), whereas total peak height changes are easily detectable. The percent relative intensity increase can be estimated by

$$\%I(t) = \frac{I(t) - I_0}{I_{max} - I_0} \times 100 \quad (1)$$

where $I(t)$ is the raw intensity measurement at a given time, I_0 is the initial value from the first frame, and I_{max} is the final data point obtained 24 h later. The plot of $\%I(t)$ vs time for the 5 wt % clay PNC is presented in Figure 5. The growth kinetics of the peak intensity can be described by

$$I(t) = I_{max}[1 - \exp(-kt)] \quad (2)$$

where k is the rate of increase of $I(t)$. $I(t)$ and I_{max} are taken as percentages; therefore, I_{max} is always 100.

The variation of the peak intensity at 2.5° with time is characterized by two parameters: k and t_c. k describes the rate with which the intensity of the peak increases in time, and t_c is a characteristic time which represents the time at which the slope of the initial linear increase intersects the slope of the final linear pseudoplateau at long time (time needed to start approaching equilibrium).

Since the intensity is related to the concentration of the intercalated stacks of d-spacing = 3.5 nm, k is related to the polymer chain diffusion inside the galleries of the organoclay, which increases the concentration of the intercalated stacks. Therefore, one expects that the variation of the concentration with time would obey a relation similar to eq 2, involving the diffusion coefficient D instead of k. However, to extract the coefficient D, one should quantitatively know the proportionality coefficient between the intensity and concentration, which is not trivial in our case. The only conclusion that can be driven from such comments is that k should be independent upon concentration as it is the case for D.

Time-resolved XRD data were obtained for hybrids containing different clay concentrations. The overall response is the same: a peak that develops at $2\theta = 2.5°$ and an unchanged secondary peak at $2\theta = 5.1°$. What changes is the relative intensity of the diffraction peaks as a function of clay concentration by dilution effect. The normalized results in $\%I(t)$ are reported in Figure 6. The parameters k and t_c obtained through eq 2 are very similar for the different PNCs, having an average value of $k \approx 4.39 \times 10^{-5}$ s^{-1} and $t_c \approx 22\,500$ s ≈ 6.25 h, in accordance with our previous discussion about the independency of k upon concentration. This suggests that the structure development occurs in much the same way despite the variations in the amount of solid particles. The rate of penetration of the clay stacks by the polymer melt seems to be unaffected by the amount of clay agglomerates in the system.

It can be assumed that at the beginning of the test a portion of the melt polymer chains have penetrated the initial clay agglomerates and that individual stacks are surrounded by the remaining chains. Diffusion of the polymer chains within the clay galleries[11,21] and the formation of a gel-like network by the clay particles are considered as responsible for structure formation. Overall, XRD data obtained for DGEBA/clay PNCs during the early stages of morphology development under quiescent conditions indicate that important structural changes occur in the scattering elements, i.e., the solid particles. The flow properties of the resulting particulate suspension have been probed simultaneously by rheological techniques, as described below.

3.2. Rheology Data. Figure 7 shows the rheology data obtained simultaneously with the XRD analyses to follow structure build-up. Both the storage (G') and the loss (G'') moduli grow over time, similarly to the diffracted intensity signal, reaching a relatively steady-state value after about 12 h. While the matrix shows a nearly Newtonian behavior with $G'' \gg G' \sim 0$, the clay−polymer system, shows an increase in G' over time before reaching a finite and constant value, with a magnitude that is 100 times higher than G' of the matrix. G'' also increases and becomes quite 2 times higher than that of the pure matrix due to enhanced local frictions and viscous dissipation induced by the presence of clay stacks. G' of the PNC is still lower than the G'', but the difference between the two was drastically reduced.

The rheological signature of the structure developed at the end of the 12 h time sweep test is shown in Figure 8. It is clear that the dynamic moduli the PNC are much higher than those of the pure matrix by many orders of magnitude both at low and high frequency ranges. While the matrix exhibits a terminal zone behavior, the PNCs show some relaxation

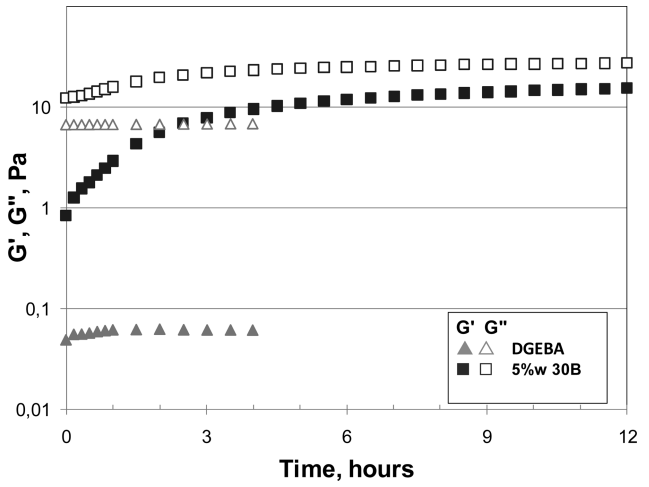

Figure 7. Time-dependent behavior of moduli for DGEBA and a PNC with solid fraction of 5 wt % (time sweep at $\omega = 1$ rad/s, $\gamma = 1\%$ for the PNC, and $\gamma = 10\%$ for the matrix alone).

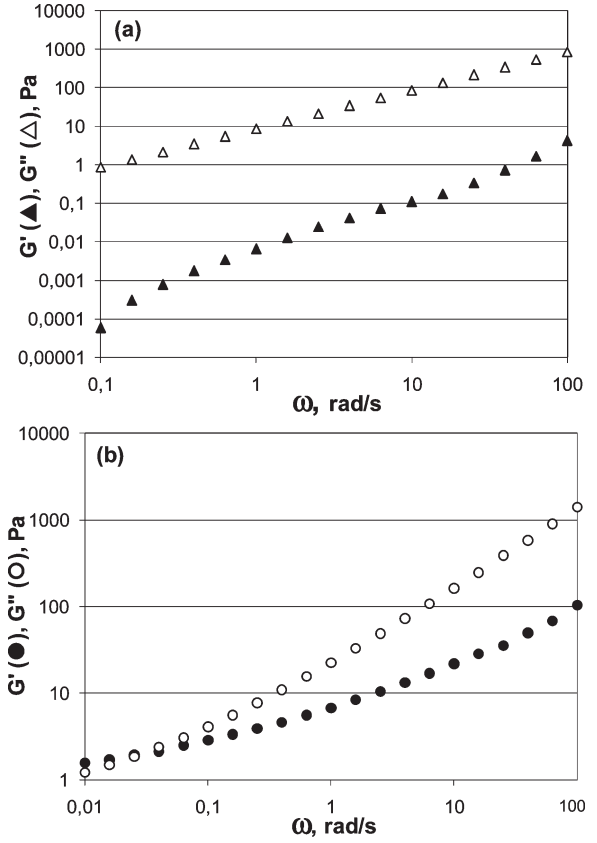

Figure 8. Storage and loss moduli vs angular frequency for (a) DGEBA and (b) 5 wt % clay PNC (frequency sweep at $\gamma = 1\%$ for the PNC and $\gamma = 10\%$ for the matrix alone). Data obtained at the end of the time sweep test (Figure 7).

process and elastic properties with the appearance of the beginning of a pseudoplateau in G' at low frequency range that starts to take over G''. This is a signature of some medium range structure build-up with some percolation between the clay stacks, similar to the percolation reported for any filled polymer.[22] The study of long-range structure would be better seen at very low frequencies, below 0.01 rad/s, but our aim here is rather to evidence the polymer dynamics and the intercalation of the organoclay galleries by diffusion of the polymer chains.

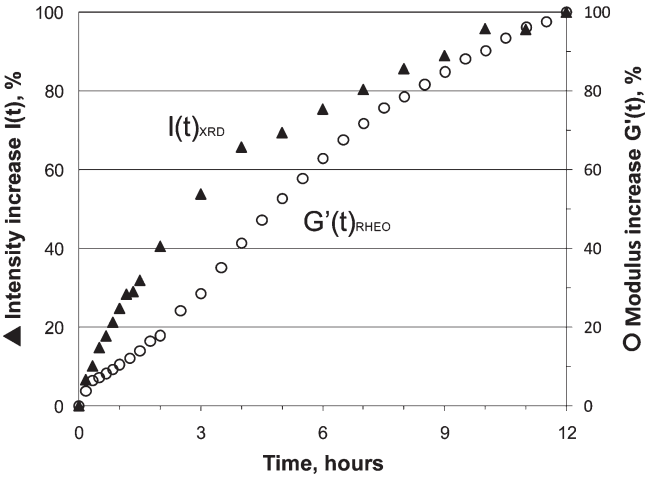

Figure 9. Corresponding percent increase of diffracted intensity and elastic modulus over a time range of 12 h for a 5 wt % clay PNC (rheological data from Figure 7 transformed according to eq 1; XRD data taken from Figure 4).

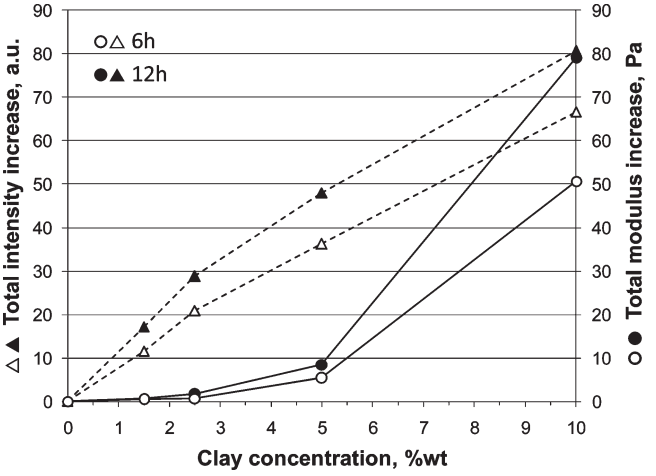

Figure 10. Corresponding increase of diffracted intensity and elastic modulus as a function of clay concentration [$I(t) - I_0$ and $G'(t) - G'_0$ for $t = 6$ and 12 h].

3.3. Rheo-XRD Data Integration: Portrait of Morphology Development. Figure 9 reports a comparison between the increase in G' and that of the diffracted intensity over a time range of 12 h for 5 wt % PNC. The two signatures (XRD and G') show the same increase trend in time. However, XRD signature is more sensitive, mainly for short times, where the variation in G' is preceded by an incubation period before showing a clear increase in time. This is because any small change in the number of expended stacking is reflected in the intensity of the diffracted X-ray spectra which depend in a very sensitive manner on concentration of ordered structures and on their intercalation, whereas the variation in the storage modulus requires an important increase in stacking concentration to be detected. Roughly speaking, G' variation with concentration in classical filled polymers can be described by $G' = G'_m(1 + A\phi + B\phi^2 + O(\phi^3))$, where A is a function of the shape factor of the dispersed filler (equal to 2.5 for isotropic fillers) and B is a complex function of the dispersed phase concentration, and it is related to matrix−clay interactions and clay stack−stacks interactions.[16,23] These two effects depend directly upon the total surface area of the dispersed lamellae. If ϕ is very small, the variation in G' remains small unless some dispersion of the agglomerates (stacks) or delamination of the lamellae is taking place, which would

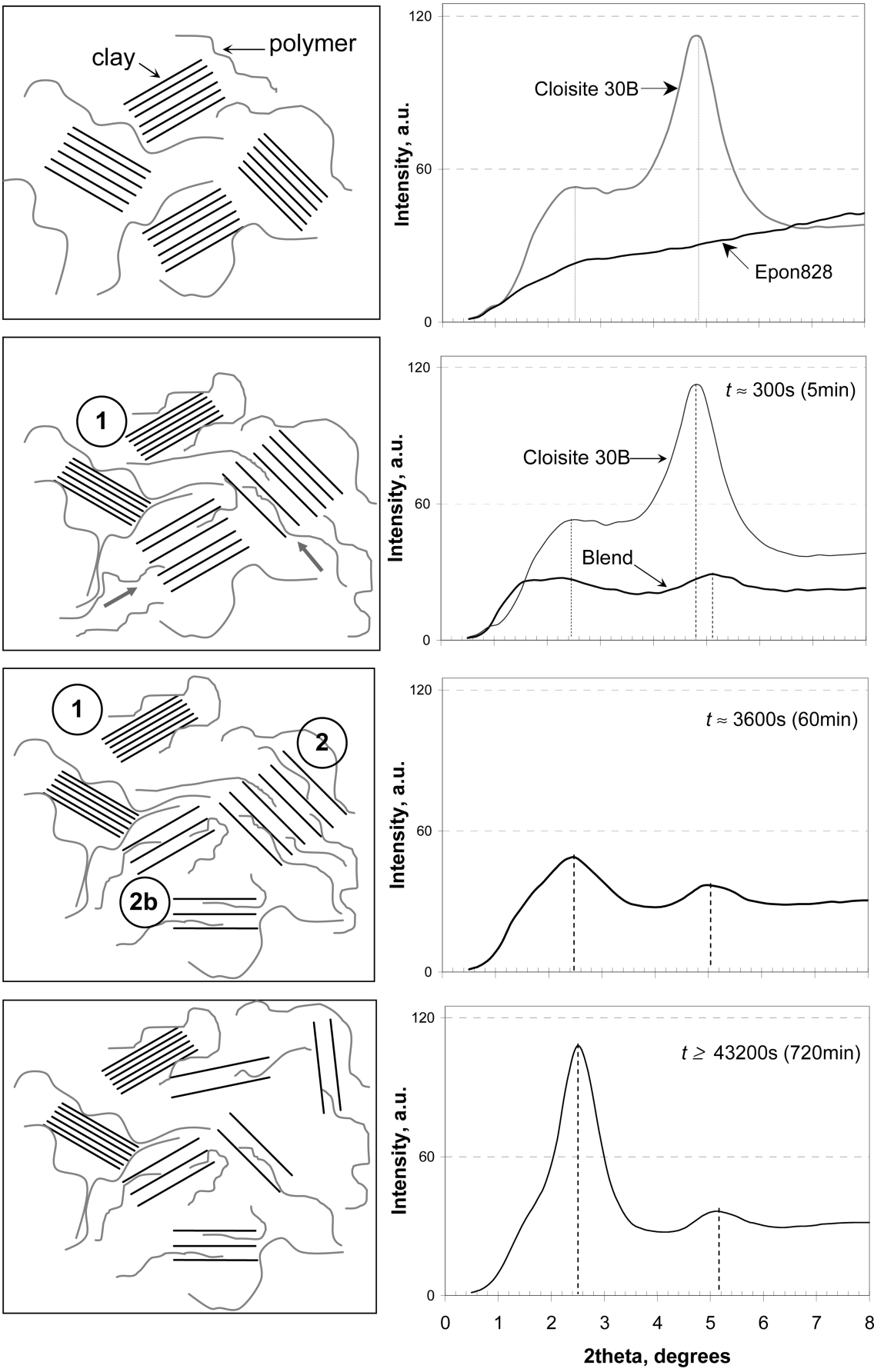

Figure 11. Suggested portrait of morphology development issued from the interpretation of rheo-XRD data (see the text for details).

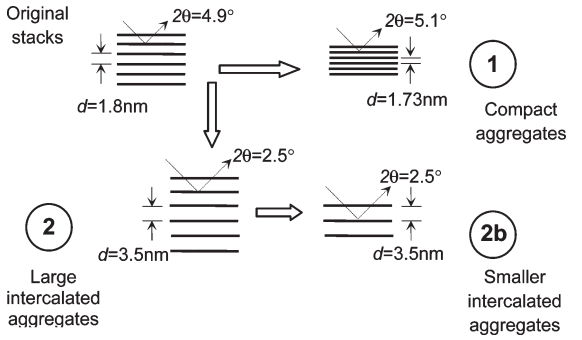

Figure 12. Suggested portrait of morphology development: changes in interlamellar spacing of clay stacks.

be better seen at very low frequencies. The diffracted-intensity curve reflects the changes going on in the clay domains by intercalation and splitting of the stacks domains, while the elastic modulus detects the evolution of the matrix properties resulting from the incorporation of the clay and the development of the matrix−filler interface and the formation of a particulate network structure.

Figure 10 compares the overall increase in the diffracted intensity and the elastic modulus at a given time as a function of clay concentration [$I(t) - I_0$ and $G'(t) - G'_0$ for $t = 6$ and 12 h]. The trend displayed by the diffracted-intensity data suggests a saturation profile, which means that the clay domains may experience spatial hindrance in concentrated PNCs. In contrast, the elastic properties rise as the filler concentration increases and as the number of the intercalated stacks increases. The evolution of parameters over time confirms the observations drawn from Figure 9, with an incubation period that depends on the dispersed phase concentration.

Rheo-XRD data have been integrated to provide the following portrait of morphology development under quiescent conditions, illustrated in Figure 11. First, the polymer chains diffuse in the agglomerates, surrounding the individual stacks. Then, the polymer molecules diffuse into the stack galleries, producing an increasingly intercalated system. Two clay populations develop during this process (denoted 1 and 2 in Figures 11 and 12). A certain amount of stacks are wrapped by the melt and do not become intercalated due to the smaller intergallery spacing (1); this fraction of clay generates the secondary peak observed in Figure 4. The intercalated stacks (2) break apart into smaller aggregates with smaller number of lamellae per stack, resulting in a growing number of scattering elements (2b), which results in an increase of the diffraction XRD peak intensity over time and a narrowing of the width of the peak. The stacks distributed in the matrix arrange in a short-range percolating network, attracted by dispersion forces, and form a colloidal suspension.

4. Concluding Remarks

PNCs offer various potential applications provided a precise control of not only the dispersion−intercalation−exfoliation and special distribution steps of the organically modified clay dispersed in a polymeric matrix but also the stability of such structure whenever the material is brought at high temperature. The experiments conducted in this work on Cloisite 30B dispersed in a Newtonian liquid showed through *in situ* XRD during SAOS tests that the structure evolves in time due to both polymeric chains diffusion within the intergallery spacing and the diffusion of the clay stacks to form an intercalated structure. For the case studied in this work, it was found that the diffusion process leads to a bimodal structure involving intercalated and wrapped stacks of lamellae by the polymeric chains. The dynamics of such intercalation process was found to be characterized by a parameter k that is related to the polymer chain diffusion within the organoclay galleries. Such a parameter was found to be independent of concentration, and therefore it somewhat describes the diffusion coefficient of the polymer chains.

The diffusion driven intercalation process examined in this work was found to increase the concentration of the intercalated stacks, to narrow their distribution, and to decrease the number of lamellae per stack.

Acknowledgment. Thanks are due to S. Pouliot and M. Rousseau for their help with the XRD and rheology equipments and for their collaboration in the development of the homemade shearing device.

References and Notes

(1) Utracki, L. A. *Clay-Containing Polymeric Nanocomposites*; RAPRA Technology Ltd.: Shawbury, England, 2004; Vols. *1* and *2*.
(2) Chavarria, F.; Shah, R. K.; Hunter, D. L.; Paul, D. R. *Polym. Eng. Sci.* **2007**, *47* (11), 1847–1864.
(3) Lertwimolnun, W.; Vergnes, B. *Polym. Eng. Sci.* **2007**, *47* (12), 2100–2109.
(4) Borse, N. K.; Kamal, M. R. *Polym. Eng. Sci.* **2006**, *46* (8), 1094–1103.
(5) Kim, S. W.; Jo, W. H.; Lee, M. S.; Ko, M. B.; Jho, J. Y. *Polym. J.* **2002**, *34* (3), 103–111.
(6) Cho, J. W.; Paul, D. R. *Polymer* **2001**, *42* (3), 1083–1094.
(7) Dennis, H. R.; Hunter, D. L.; Chang, D.; Kim, S.; White, J. L.; Cho, J. W.; Paul, D. R. *Polymer* **2001**, *42* (23), 9513–9522.
(8) Fornes, T. D.; Yoon, P. J.; Keskkula, H.; Paul, D. R. *Polymer* **2001**, *42* (25), 9929–9940.
(9) Ray, S. S.; Bousmina, M.; Okamoto, M. *Macromol. Mater. Eng.* **2005**, *290* (8), 759–768.
(10) Ray, S. S.; Bousmina, M. *Polymer* **2005**, *46* (26), 12430–12439.
(11) Bousmina, M. *Macromolecules* **2006**, *39* (12), 4259–4263.
(12) Lele, A.; Mackley, M.; Galgali, G.; Ramesh, C. *J. Rheol.* **2002**, *46* (5), 1091–1110.
(13) Homminga, D.; Goderis, B.; Hoffman, S.; Reynaers, H.; Groeninckx, G. *Polymer* **2005**, *46* (23), 9941–9954.
(14) Panine, P.; Gradzielski, M.; Narayanan, T. *Rev. Sci. Instrum.* **2003**, *74* (4), 2451–2455.
(15) Pople, J. A.; Hamley, I. W.; Diakun, G. P. *Rev. Sci. Instrum.* **1998**, *69* (8), 3015–3021.
(16) Bousmina, M.; Aouina, M.; Chaudhry, B.; Guenette, R.; Bretas, R. *Rheol. Acta* **2001**, *40* (6), 538–551.
(17) Deyrail, Y.; Huneault, M.; Bousmina, M. *J. Polym. Sci., Part B* **2009**, *47* (15), 1467–1480.
(18) Deyrail, Y.; Huneault, M.; Bousmina, M. *J. Rheol.* **2007**, *51* (5), 781–797.
(19) Kádár, F.; Százdi, L.; Fekete, E.; Pukánszky, B. *Langmuir* **2006**, *22* (12), 7848–7854.
(20) Kong, D.; Park, C. E. *Chem. Mater.* **2003**, *15* (2), 419–424.
(21) Vaia, R. A.; Jandt, K. D.; Kramer, E. J.; Giannelis, E. P. *Macromolecules* **1995**, *28* (24), 8080–8085.
(22) Bousmina, M.; Muller, R. *J. Rheol.* **1993**, *37* (4), 663–679.
(23) Eslami, H.; Grmela, M.; Bousmina, M. *J. Rheol.* **2007**, *51* (6), 1189–1222.